The 2015 World Congress on
Advances in Civil, Environmental, and Materials Research (ACEM15)
Incheon, Korea, August 25-29, 2015

Seismic Behavior of Full-Scale Beam-Column Knee Joints

*Byung Un Kwon[1)], Ah Sir Cho[2)], Tae-Soo Oh[3)], and Thomas Kang[4)]

[1), 2), 4)] *Department of Architecture & Architecture Engineering, Seoul National University, Seoul, Korea*
[3)] *Daewoo Engineering and Construction Co., Ltd., Suwon, Korea*
[4)] *tkang@snu.ac.kr*

ABSTRACT

Beam-column joint is a structurally important element especially in high seismic zones. In 2002, Joint ACI-ASCE Committee 352 published the ACI 352R-02 guides for the design of reinforced concrete beam-column joints, and now the knee joint part needs to be updated because of the addition of recent data that expand the limited database. The purpose of this study is to help update ACI 352R-02 by investigating the seismic behavior of beam-column knee joints subjected to reversed-cyclic loading with several key parameters (e.g. high strength materials, post-tensioning) that have not been studied before. For this, six specimens were tested. Test results show that all the specimens showed very ductile behavior and proper energy dissipation capacities. Particularly, post-tensioned concrete knee joint specimens with very high joint shear demands achieved excellent seismic performance.

1. INTRODUCTION

The beam-column joint is one of the most structurally important parts in the moment frame which primarily resists lateral forces due to earthquake actions. To promote ductile performance of the moment frame under seismic forces, plastic hinges should be formed at the end of the beam before column hinging according to the strong column/weak beam design concept. Also, for ductile behavior, proper seismic details of beam-column joints should be provided. Joint ACI–ASCE Committee 352 publication of ACI 352R-02 (2002) provides guidelines for the design of beam-column joints; however, ACI 352 guideline is in need of updates for several parts.

In congested exterior beam-column joints, using headed-bars for anchoring the beam bars into joint area is efficient way. Conventionally, 90 degree hooked bars which causes steel congestion, time-consuming fabrication, and improper concrete placement are used. Such a congestion problem gets even worse in knee beam-column joints as

---

[1), 2)] Graduate Student
[3)] Engineer
[4)] Associate Professor

the column bars should also be anchored in the joint. Despite many advantages of headed reinforcement, current code provisions and recommendations have insufficient details regarding the headed bars. In this study, the effects of the headed bars for the seismic behavior of various types of knee joints were investigated experimentally.

Recently, the use of high-strength concrete and steel is increasingly popular because of its several advantages. In the current design guides including ACI 352R-02, there are limitations on material properties. ACI 352R-02 recommends that concrete compressive strength and yield strength of reinforcing bars are valid for up to 100 MPa and 540 MPa, respectively. These limitations may need to be extended as there are growing needs in the industry; however, there is a lack of available experimental data to confirm the effects of using high-strength materials.

Furthermore, the post-tensioning (PT) method was adopted in this study, which might improve structural integrity of a member. However, ACI 352R-02 and current ACI 318-11 (2011) codes do not provide details for PT beam-column joints. This is due to the scarcity of previous research on the performance of beam-column joints with post-tensioning tendons. Fig. 1 shows the headed bars and unbonded tendons with fixed end anchors.

Fig. 1 Headed bars and unbonded tendons with PT anchors

2. TEST PROGRAM

2.1 Specimens Design

Five full-scale specimens were designed and constructed according to ACI 352R-02 recommendations. ‘K-RC-N’ was a reference specimen that consists of normal-strength concrete (35 MPa) and SD400 (yield strength = 400 MPa) reinforcement while high-strength concrete (80 MPa) and SD600 (yield strength = 600 MPa) bars were used to fabricate ‘K-RC-H’. Four unbonded tendons were applied to three PT specimens; ‘K-PT-N-1’, ‘K-PT-N-2’, and ‘K-PT-N-3’.

The difference among the PT specimens was the number of beam longitudinal bars that would affect the joint shear demand directly. The joint shear demand for knee joints is expressed as tensile force at the critical section of the beam (i.e., beam-column interface). For convenient comparison, the tensile force was calculated by dividing the

beam moment by the same moment arm length of 0.9*d* for all specimens including PT specimens though the tendon had the smaller effective depth. Here, *d* is the effective depth of tensile reinforcing bars. Nominal joint shear strength can be calculated based on ACI 352R-02. All the PT specimens had the same value of the joint shear strength because the effective joint area and concrete strength were the same.

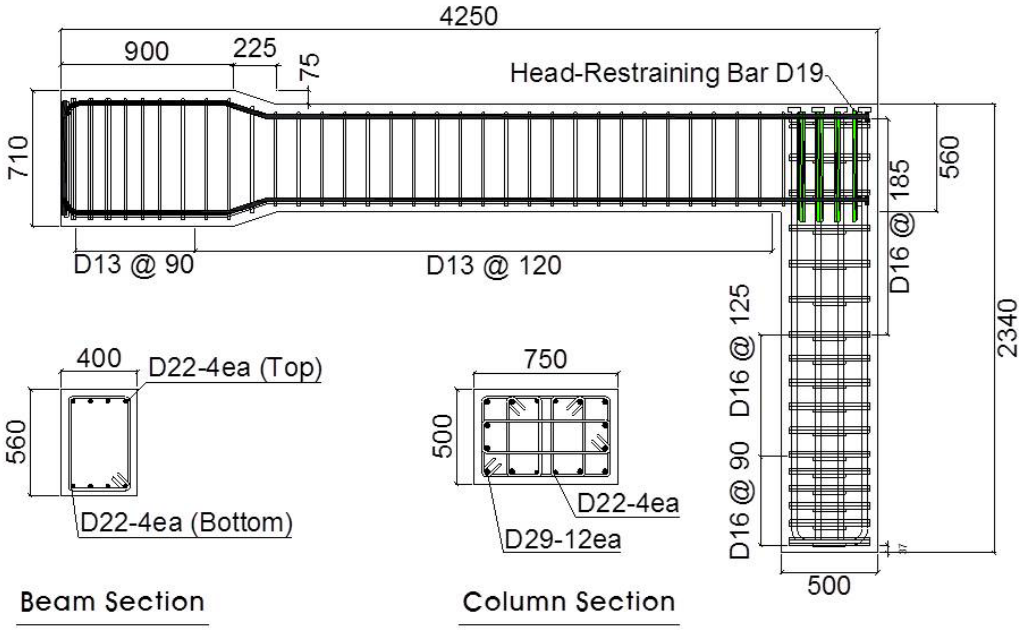

(a) K-RC-H

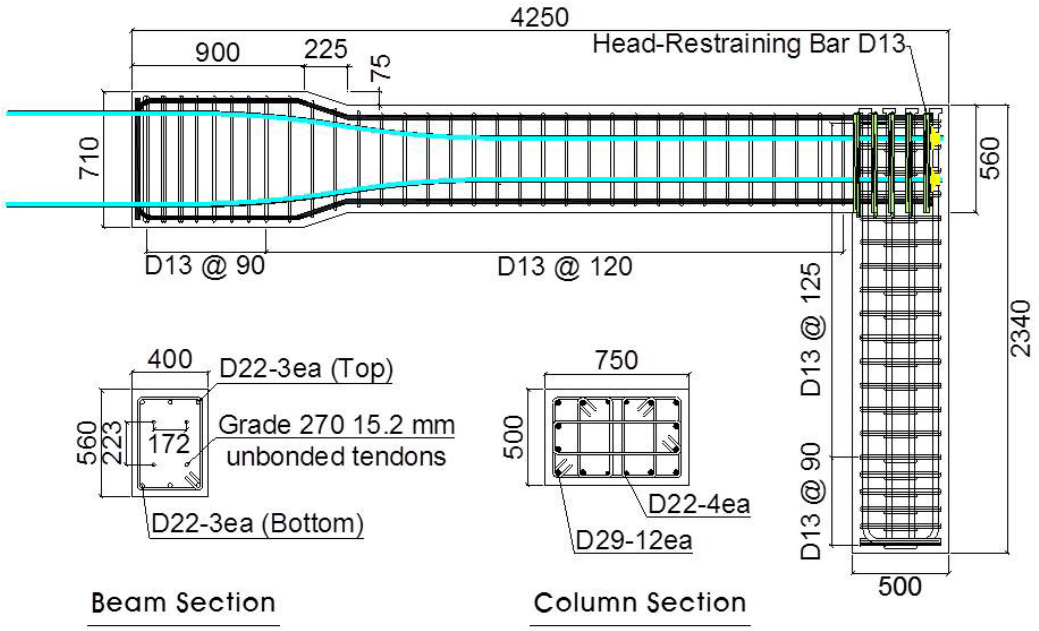

(b) K-PT-N-1

Fig. 2 Drawings of test specimens

For all top and bottom reinforcing bars, the headed bars were used for anchorage in the joint. Details of heads (e.g., size, ratio of the net head section area to the cross-section area of bar) and reinforcement in the joint area (e.g., development length, clear spacing between headed bars) were determined based on the previous researches (Wallace 1998; Chun 2007; Kang 2010; Kang 2012). Figure 2 shows the drawings of 'K-RC-H' and 'K-PT-N-1', and the comparison of the beam sections of PT specimens is shown in Fig. 3. The dimensions and other details of the specimens are summarized in Tables 1 and 2, respectively.

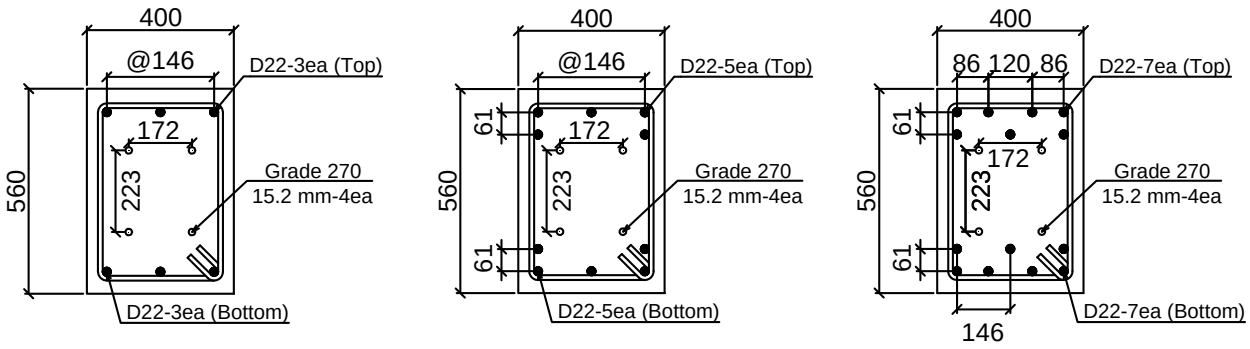

(a) K-PT-N-1 (b) K-PT-N-2 (c) K-PT-N-3

Fig. 3 Beam sections of 'K-PT-N-1', 'K-PT-N-2', and 'K-PT-N-3'

Table 1 Dimension of specimens

Specimen	Beam			Column	
	Size (mm)	Bars	Tendons	Size (mm)	Bars
K-RC-N	400×560	D22×4	-	500×750	D22×4, D29×12
K-RC-H	400×560	D22×4	-	500×750	D22×4, D29×12
K-PT-N-1	400×560	D22×3	Grade 270×4	500×750	D22×4, D29×12
K-PT-N-2	400×560	D22×5	Grade 270×4	500×750	D22×4, D29×12
K-PT-N-3	400×560	D22×7	Grade 270×4	500×750	D22×4, D29×12

Table 2 Details of specimens

Specimen	f_c' (MPa)	f_y (MPa)	V_u (kN)	V_n (kN)	$l_{dt(pro)}$ (mm)	$l_{dt(req)}$ (mm)	$l_{dt(pro)}$ / $l_{dt(req)}$
K-RC-N	35	400	804	1129	397	285	1.39
K-RC-H	80	600	1239	1708	393	283	1.39
K-PT-N-1	35	400	858	1129	397	283	1.40
K-PT-N-2	35	400	1140	1129	397	283	1.40
K-PT-N-3	35	400	1536	1129	397	283	1.40

f_c': design concrete compressive strength; f_y: design yield strength of reinforcement; V_u: design joint shear demand; V_n: joint nominal shear strength; $l_{dt(pro)}$: provided development length; $l_{dt(req)}$: required development length for headed bars (ACI 352R-02)

Table 3 Details of materials (Unit: MPa)

Normal Strength Concrete			**High Strength Concrete**			**SD400 (D22)**		**SD600 (D22)**	
f'_c	f'_{c_actual}	f_t	f'_c	f'_{c_actual}	f_t	f_y	f_{y_actual}	f_y	f_{y_actual}
35	41.3	5.4	80	103.4	9.2	400	474	600	675

f'_{c_actual}: actual concrete compressive strength; f_t: concrete tensile strength; f_{y_actual}: actual yield strength of reinforcement

2.2 Materials

Measured material properties are listed in Table 3. Specimen 'K-RC-H' was constructed with 80 MPa concrete and SD600 steel. For high-strength concrete, the mixture proportions were carefully designed, and Zirconium was added to gain the long-term strength and reduce the heat of hydration. As a result, the strength of 80 MPa was successfully achieved, and the measured strength was 100.3 MPa. SD600 steel was used for the reinforcing bar, and yield and tensile strengths were measured about 650 MPa and 780 MPa, respectively. The unbonded PT tendons were the 15.2 mm diameter seven-wire strands of Grade 270 (1860 MPa), and measured tensile strength was 1776 MPa.

2.3 Loading History

All knee joint specimens were tested in upright position. A hydraulic actuator having capacity of 100 kN was placed at the end of the beam section. Its maximum stroke length was ± 250 mm. The loading history was planned to have displacement control according to ACI 374.2R-13 (2013). The tests were conducted from the drift level of 0.35% to that of over 5% with assumption that the drift at yielding point would be 0.7%. Each drift level had 2 cycles including displacement peaks in both positive (push) and negative (pull) directions. Without complete specimen failure, the test was finished when the actuator reached the maximum stroke. The test setup and loading history are shown as Fig. 4.

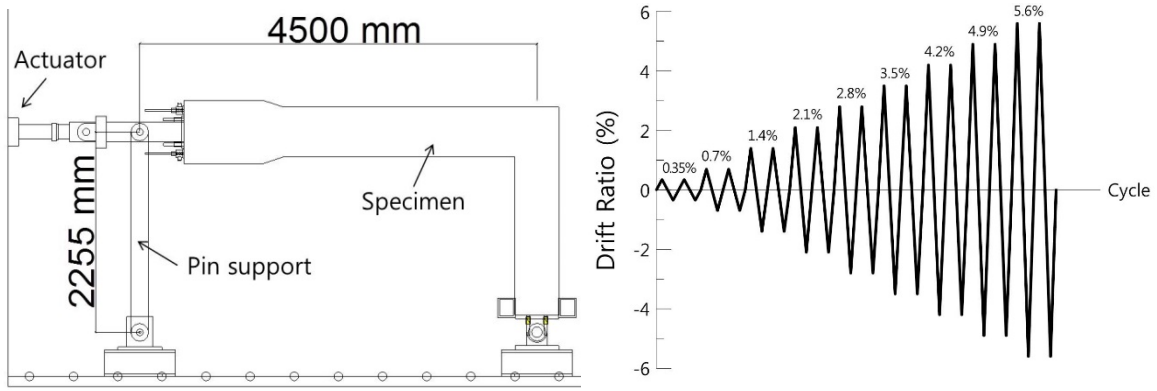

Fig. 4 Test setup and loading history

3. TEST RESULT

3.1 Moment-Drift Ratio

Test results regarding moment and drift ratio are summarized in Table 4. Moment-drift ratio curves are shown in Fig. 5, where red lines stand for nominal moment value (M_n) calculated based on ACI 318-11 with measured material properties.

Table 4 Test results

Specimen	M_y	M_n	M_{peak}	V_{u_a}	V_{n_a}	V_{u_a}/V_{n_a}	θ_y	θ_{peak}	θ_{max}	μ
K-RC-N	282	387	425	952	1232	0.77	1	6.2	8.8	8.8
K-RC-H	258	381	486	1396	1950	0.72	1.4	5.6	5.6	4
K-PT-N-1	307	352	469	1050	1232	0.85	1.3	5.3	8.7	6.7
K-PT-N-2	355	504	613	1374	1232	1.11	1.2	8.8	9.4	7.8
K-PT-N-3	507	652	715	1602	1232	1.3	1.9	3.6	9.4	4.9

M_y: moment at yielding; M_n: nominal moment (calculated based on ACI 318-11 with measured material properties); M_{peak}: measured peak moment; V_{u_a}: maximum joint shear demand; V_{n_a}: nominal joint shear strength; θ_y: drift ratio at M_y; θ_{peak}: drift ratio at M_{peak}; θ_{max}: maximum drift ratio; μ: ductility (θ_{max}/θ_y); Moment unit: kN-m; Shear unit: kN; Drift ratio unit: %

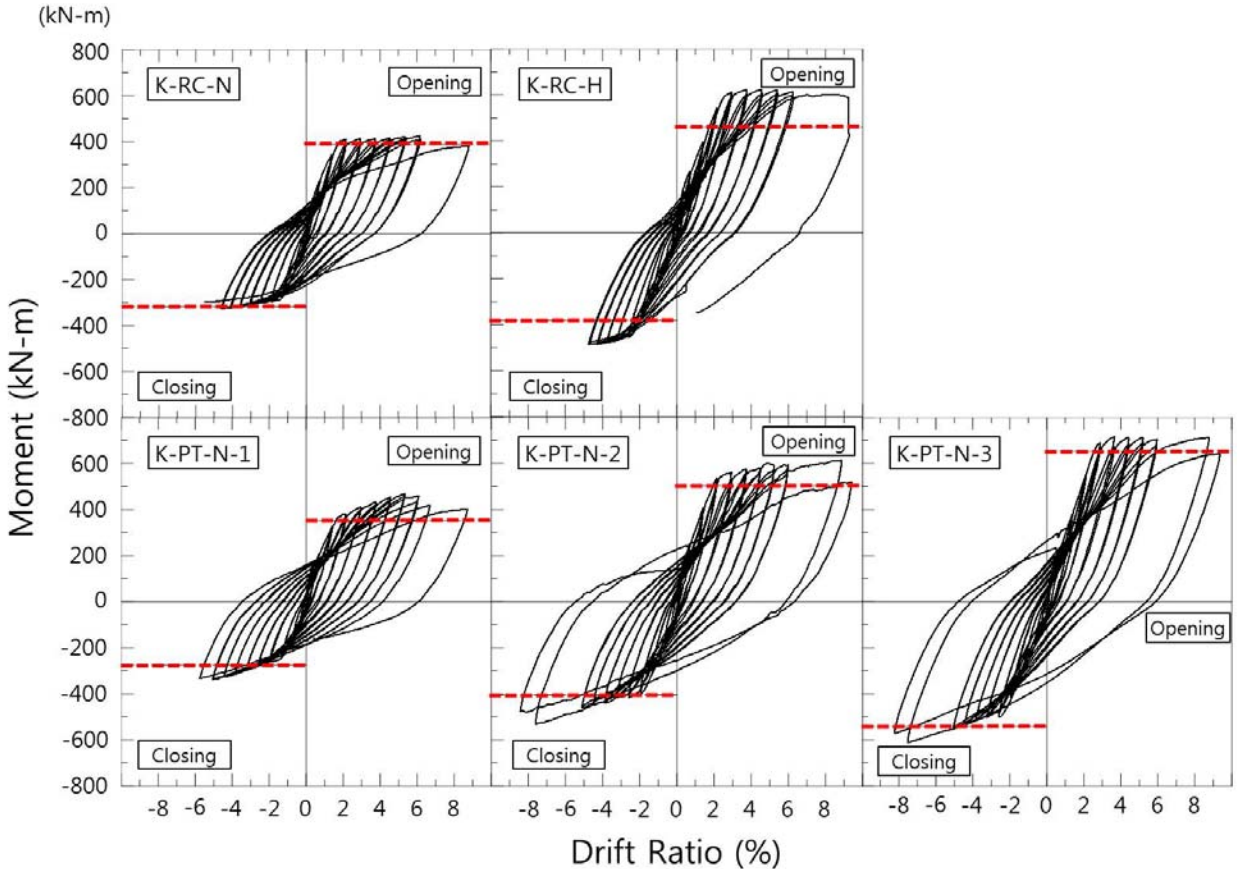

Fig. 5 Moment-drift ratio curves

All test specimens showed excellent seismic performance with highly ductile and hysteretic behavior. While the drift increased, the moderate strength degradation was

negligible from the curves. 'K-RC-H' with high-strength materials had equally excellent ductility and energy dissipation for the specimen having the normal-strength concrete. The PT specimens also showed excellent seismic performance. Even 'K-PT-N-2' and 'K-PT-N-3' were designed to have very high joint shear demand-to-strength ratios, the strength reduction occurred only at the final cycles. Due to the effect of post-tensioning, applied moment values were increased beyond the yield of beam top/bottom reinforcing bars. Without pinching, the shape of curve indicates that energy dissipation capacity was excellent. The peak moment (M_{peak}) was larger than nominal moment (M_n) by 10 to 35%. The yield moment (M_y) and yield drift ratio (θ_y) were obtained based on the point when tensile reinforcement began to yield according to the strain gauge data. Ductility (μ) values of the specimens ranged from 4 to 10.5, and 'K-RC-H' had the lowest ductility of 4.

3.2 Failure Mode and Crack Pattern

All specimens failed in ductile flexure manner and the flexure failure was focused on the critical section of the beam member without or prior to joint failure. Until the end of test, the beam-column joints maintained their lateral resistance capacity without apparent loss, though severe cracks occurred around the beam near the beam-column interface at 2.8~3.5% drift levels. Except for 'K-RC-H', concrete cover at the critical section was substantially spalled off at the final stage of the experiment. Compared to 'K-RC-N' having low shear strength ratio, some cracks occurred on the backside of joint after 2.8% drift levels. Figure 6 show the final crack patterns of 'K-RC-N', 'K-RC-H', and 'K-PT-N-3'.

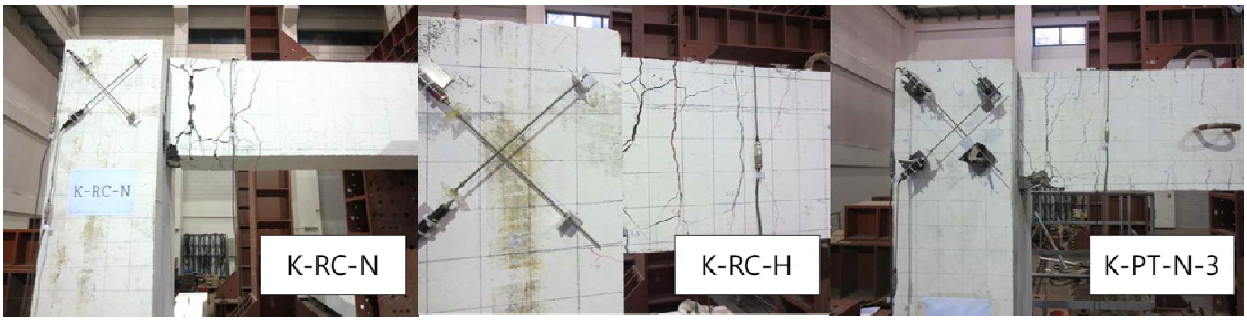

Fig. 6 Final crack patterns

3.3 Joint Shear Distortion

Joint shear distortion was obtained using the measured data from LVDTs which were diagonally placed on the joint surface. The joint shear distortions were quite small. Figure 7 plots the joint shear force normalized by the nominal joint strength versus the joint shear distortion. Compared with other specimens, the joints of 'K-PT-N-2' and 'K-PT-N-3' were subjected to the joint shear forces larger than the nominal joint shear strengths and experienced larger joint shear distortions, which were still modest and did not adversely affect the overall joint performance. This indicates that the post-tensioning improved the joint shear strength significantly and the actual joint shear strength of PT knee joints was much larger than that of comparable reinforced concrete knee joints. This should be considered when updating ACI 352R-02 and ACI 318-14.

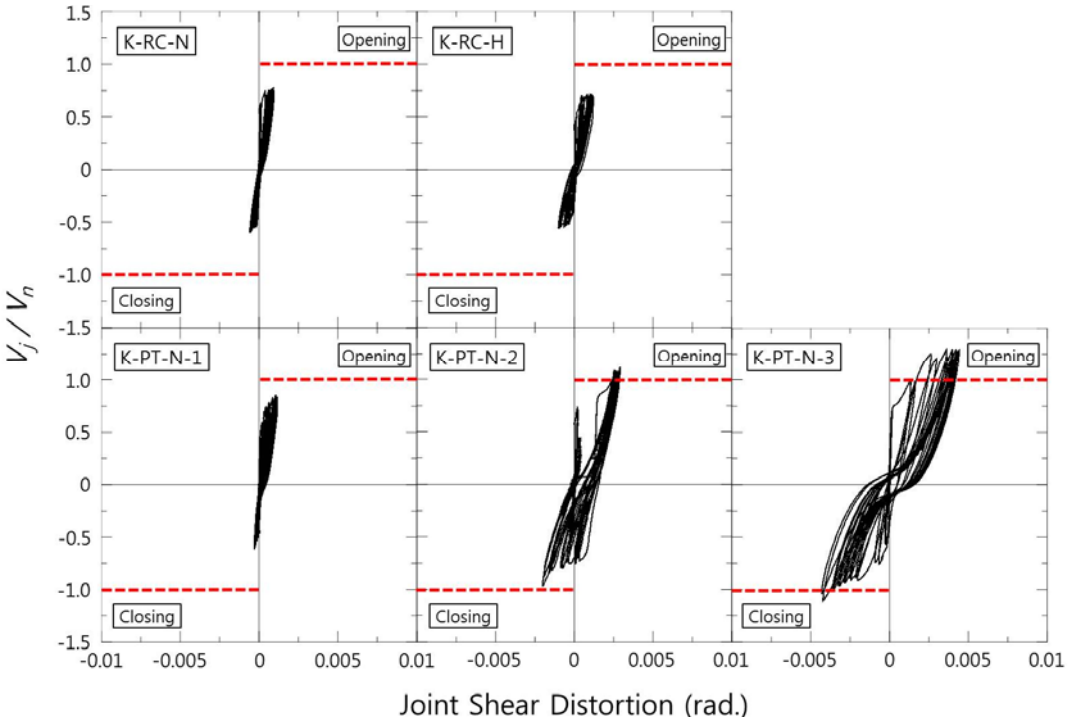

Fig. 7 Joint shear force - joint shear distortion curves

3.4 Reinforcement Yielding

Strain gauges were attached to the beam longitudinal bars, transverse hoops and tie, and U-stirrups. Based on material tests, the strain at the yielding point was about 0.002. For beam top/bottom bars, strain gauges were attached on the critical section and the location in front of the head. For all specimens, the strain at the critical section was much higher than that at the head. After about 2.8% drift, yielding occurred at the beam-column interface though no specific yielding was observed near the head until the end. This indicates that bonding between the reinforcement and concrete was not deteriorated much during the testing and the headed bars were well anchored. Figure 8 plots the strains of beam bottom bars of 'K-RC-N', 'K-RC-H', and 'K-PT-N-3'.

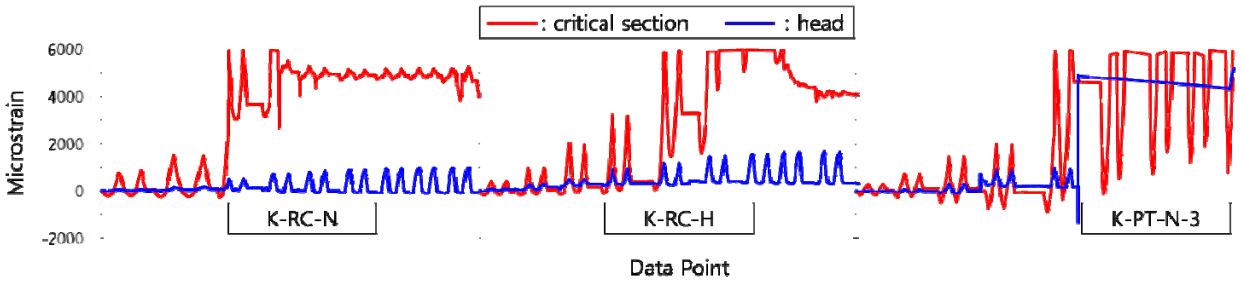

Fig. 8 Strains of beam bottom bars of 'K-RC-N', 'K-RC-H', and 'K-PT-N-3'

4. CONCLUSIONS

Seismic behavior of five full-scale beam-column knee joints including one with high-strength concrete and three with unbonded PT tendons were experimentally investigated. The specimens with varied joint shear demand-to-strength ratios were applied according to ACI 352R-02, and tested in accordance with ACI 374.2R-13. Based on the test results, the preliminary conclusions are as follows:

1. Beam-column knee joints showed desired failure pattern (beam flexural failure followed by modest joint deterioration) and excellent seismic performance such as large lateral load-drift hysteretic loop, ductility and energy dissipation.

2. The seismic performance of 'K-RC-H' with high-strength materials is also equivalent or comparable to that of 'K-RC-N'. This indicates that the use of SD600 steel is promising when used with 80~100 MPa concrete as special moment frames.

3. Post-tensioned specimens did not fail until the end of testing. Moreover, energy dissipation capacities were excellent likely due to the enhanced structural integrity provided by post-tensioning.

4. Although two post-tensioned specimens of 'K-PT-N-2' and 'K-PT-N-3' were designed with very high joint shear demands, their relatively large joint shear distortions did hardly affect the overall behavior of the specimens. This indicates that the joint shear strength of post-tensioned joints is larger than that of conventional reinforced concrete joints.

5. ACKNOWLEDGMENTS

This research was supported by a grant (13SCIPA02) from Smart Civil Infrastructure Research Program funded by Ministry of Land, Infrastructure and Transport (MOLIT) of Korea government and Korea Agency for Infrastructure Technology Advancement (KAIA).

REFERENCES

ACI Committee 318 (2011), *Building Code for Structural Concrete and Commentary (ACI 318M-11)*, American Concrete Institute, Farmington Hill, MI.

ACI Committee 374 (2013), *Guide for Testing Reinforced Concrete Structural Elements under Slowly Applied Simulated Seismic Loads (ACI 374.2R-13)*, ACI.

Joint ACI-ASCE Committee 352 (2002), *Recommendation for Design of Beam-Column Connections in Monolithic Reinforced Concrete Structures (ACI 352R-02)*, ACI.

Chun, S.C., Lee, S.-H., Kang, T.H.-K., Oh, B., and Wallace, J.W. (2007), "Mechanical anchorage in exterior beam-column joints subjected to cyclic loading", *ACI Structural J.*, 104(1), 102-112.

Kang, T.H.-K., Ha, S.-S., and Choi, D.-U. (2010), "Bar pullout tests and seismic tests of small-headed bars in beam-column joints", *ACI Structural J.*, 107(1), 32-42.

Kang, T.H.-K., Kim, W., and Shin, M. (2012), "Cyclic testing for seismic design guide of beam-column joints with closely spaced headed bar", *J. Earthquake Eng.*, 16(2), 211-230.

Wallace, J.W., McConnell, S.W., Gupta, P., and Cote, P.A. (1998), "Use of headed reinforcement in beam-column joints subjected to earthquake loads", *ACI Structural J.*, 95(5), 590-602.